analytical chemistry

Article

Cite This: *Anal. Chem.* 2019, 91, 14631−14638

pubs.acs.org/ac

Portable Microfluidic Biosensing System for Real-Time Analysis of Microdialysate in Transplant Kidneys

Isabelle C. Samper,[‖,†] Sally A. N. Gowers,[‖,†] Marsilea A. Booth,[†] Chu Wang,[†] Thomas Watts,[†] Tonghathai Phairatana,[†,§] Natalie Vallant,[‡] Bynvant Sandhu,[‡] Vassilios Papalois,[‡] and Martyn G. Boutelle*[,†]

[†]Department of Bioengineering, Imperial College London, London SW7 2AZ, U.K.

[‡]Department of Surgery and Cancer, Imperial College London, London SW7 2AZ, U.K.

[§]Institute of Biomedical Engineering, Faculty of Medicine, Prince of Songkla University, Hat Yai 90110, Thailand

Supporting Information

ABSTRACT: Currently, there is a severe shortage of donor kidneys that are fit for transplantation, due in part to a lack of adequate viability assessment tools for transplant organs. This work presents the integration of a novel wireless two-channel amperometric potentiostat with microneedle-based glucose and lactate biosensors housed in a 3D printed chip to create a microfluidic biosensing system that is genuinely portable. The wireless potentiostat transmits data via Bluetooth to an Android app running on a tablet. The whole miniaturized system is fully enclosed and can be integrated with microdialysis to allow continuous monitoring of tissue metabolite levels in real time. We have also developed a wireless portable automated calibration platform so that biosensors can be calibrated away from the laboratory and in transit. As a proof of concept, we have demonstrated the use of this portable analysis system to monitor porcine kidneys for the first time from organ retrieval, through warm ischemia, transportation on ice, right through to cold preservation and reperfusion. The portable system is robust and reliable in the challenging conditions of the abattoir and during kidney transportation and can detect clear physiological changes in the organ associated with clinical interventions.

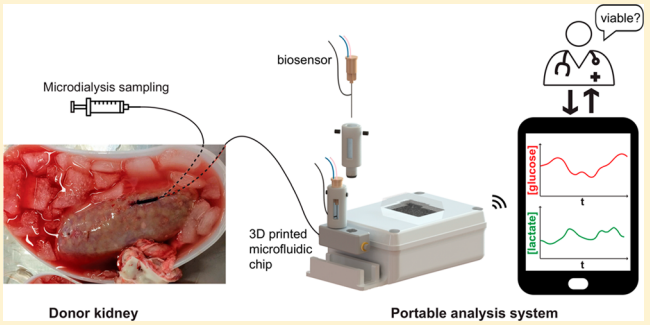

Kidney transplantation is the optimal treatment for patients with end-stage kidney disease. However, there is a huge shortage of donor kidneys worldwide; according to the Organ Procurement and Transplantation Network, there are currently 94,755 patients waiting for a kidney transplant in the United States alone and in 2018 only 21,167 kidneys transplants were carried out.[1] As a result, there is a critical need to increase the pool of available donor organs.

The majority of kidney transplants use organs from deceased donors, predominantly from donation-after-brain-death (DBD) donors, whose hearts were beating prior to retrieval as ischemic damage should be limited. However, with the need to increase the donor pool, there is considerable interest in reducing the discard rate of marginal organs, such as those from donation-after-cardiac-death (DCD) donors and expanded criteria donors (ECD). DCD organs tend to be under-utilized as there is a period of prolonged warm ischemia that can cause the organ not to function in the initial period following transplantation (delayed graft function).[2−4] ECD organs, such as those from donors who are aged 60 years and older or who do not meet specifically defined criteria,[5] are at a higher risk of graft failure;[5] however, these transplants have been shown to be beneficial compared with the alternative of chronic dialysis treatment.[6]

In order to decrease the discard rate of these marginal donor organs and hence increase the number of organs available for transplantation, there is an urgent need to improve organ viability assessment prior to transplantation so that organs that are at risk of poor outcomes can be identified early. Currently, organs are accepted or discarded based on subjective evaluation of donor characteristics and macroscopic kidney assessment only.[7] A move toward a more quantitative measure will aid in clinical decision-making and could substantially increase the use of marginal donor organs. Moreover, better viability assessment could allow better evaluation of novel preservation methods to recondition marginal organs.

Real-time chemical monitoring can provide time-critical information on tissue health in a clinical setting.[8] Microdialysis is a tissue sampling technique that uses a small (typically 600 μm diameter) probe with a semipermeable membrane at the tip. The inside of the membrane is perfused at a low flow rate

Received: August 18, 2019
Accepted: October 24, 2019
Published: October 24, 2019

DOI: 10.1021/acs.analchem.9b03774
Anal. Chem. 2019, 91, 14631−14638

(0.1−2.0 μL/min), which sets up a concentration gradient across the membrane between the extracellular fluid and the probe, creating a dialysate stream that is representative of the tissue concentrations of analytes. This sampling technique can be coupled with high-resolution analysis techniques for in vivo monitoring.[9−16] Our research groups have previously demonstrated that using online microdialysis to measure levels of glucose and lactate can be used to provide information on the metabolic state of transplant organs ex vivo and can detect metabolic differences between organs.[17] However, in this previous work, the analysis system was housed on a large clinical trolley and was therefore only suitable for lab-based monitoring. This meant that it was not possible to monitor the organs during the crucial stages immediately after retrieval. As a first step toward portable monitoring, attempts were made to collect the dialysate in fine-bore tubing to be played back later.[18] Although this enabled measurement of dialysate levels, the data was not obtained in real time.

A portable miniaturized analysis system that can be taken to the donor site to monitor tissue metabolism during the initial stages of ischemia and that can travel with the transplant organ to the recipient site would allow clinicians to track the health of the organ in real time from retrieval right through to transplantation. Microfluidics are ideally placed to reliably handle the low fluid volumes generated by microdialysis with high time resolution.[9−11,19−23] Our group has developed a 3D printed microfluidic chip that is extremely robust and reliable when coupled with microdialysis for clinical monitoring.[10]

In this study, we describe the development of a miniaturized wireless portable analysis system for continuous measurement of dialysate glucose and lactate levels in real time. The analysis system incorporates our established microneedle-based biosensors[9,11] and 3D printed microfluidic chip[10] and integrates them with a novel two-channel wireless potentiostat to form a compact monitoring system. For this study, we have also made our autocalibration system[19] wireless and portable so that biosensors can be calibrated in transit, ensuring that the system is ready to use on arrival. Here we show the use of continuous online microdialysis to measure tissue metabolite levels in real time in kidneys during the critical time period of organ retrieval for the first time, as well as during organ preservation, organ reperfusion, and simulated transplantation, demonstrating a robust and reliable analysis system for portable sensing applications.

EXPERIMENTAL SECTION

Reagents. Glucose oxidase (GOx) from *Aspergillus niger* and lactate oxidase (LOx) from *Aerococcus viridians* were purchased from Sekisui Diagnostics. Polyurethane (Texin 985) was obtained from Bayer. Other reagents were obtained from Sigma-Aldrich.

Electrode Fabrication. The biosensors used in this work are fabricated based on a combined needle electrode, which has been described in detail elsewhere.[24,25] Briefly, a 50 μm diameter platinum/iridium (90%:10%) wire insulated with polytetrafluoroethylene (PTFE, coating thickness 0.0125 mm Advent Research Materials) and a 50 μm silver wire insulated with polyester (coating thickness 0.0075 mm, Goodfellow) were threaded through a 27G hypodermic needle. The insulation layer was removed from the ends of the wires using a small flame to expose the metal, and the ends of each wire were connected to an electrical wire using conductive silver epoxy glue (RS Components). Epoxy resin (Robnor resins, CY1301 and HY1300) was used to fill the needle and to secure the wires in place. Once the epoxy resin was cured, the bevel of the needle was sanded down using sandpaper (Buehler) to create silver and platinum disc electrodes. The blunt needle was then polished sequentially with alumina slurries (1, 0.3, and 0.05 μm). Finally, in order to create the Ag|AgCl reference electrode, the tip of the needle was dipped into a potassium dichromate reference solution (BASi) for 3 s and then into a solution of 1.2 M hydrochloric acid for 20 s to remove the oxide layer from the working and counter electrodes. Cyclic voltammetry in 1.5 mM ferrocene monocarboxylate solution (Fc) was used to assess the working electrode surface.

Biosensor Fabrication. Glucose and lactate biosensors were fabricated in several layers as described previously.[9,11] (i) First, the working electrode was coated with poly(m-phenylenediamine) (mPD) using electropolymerization to screen out potential interferences. This was done by placing the needle electrode in a 100 mM solution of the m-phenylenediamine monomer in 10 mM PBS at pH 7.4. The working electrode potential was held at 0 V for 20 s, +0.7 V for 20 min to initiate electropolymerization, and finally 0 V for 3 min to stabilize the film. The electrode was gently rinsed with deionized water, and the presence of the film was verified with cyclic voltammetry in Fc solution. (ii) After successful electropolymerization of the screening layer, the electrodes were dipped into the enzyme solution; for lactate biosensors this was 60 mg/mL LOx, 30 mg/mL bovine serum albumin (BSA), 2% v/v glycerol, and 45.6 mg/mL poly(ethylene glycol) diglycidyl ether (PEG-DE) in 10 mM PBS pH 7.4, and for glucose biosensors this was 60 mg/mL GOx, 30 mg/mL BSA, 1% *v/v* glycerol, and 14.8 mg/mL PEG-DE in 10 mM PBS pH 7.4, adapted from the method described by Vasylieva et al.[10,26] The needles were placed in the oven at 55 °C for 2 h to cross-link the hydrogel layer. During operation, a potential of +0.7 V was applied to the working electrode to drive the oxidation of hydrogen peroxide produced by the reaction of the substrate with the enzyme. (iii) Finally, following enzyme immobilization, biosensors were coated with a solution of polyurethane (Texin 985, Bayer) in tetrahydrofuran by dip coating to provide a diffusion-limiting layer and hence to extend their dynamic range.[9] The sensors were allowed to dry at room temperature and then stored at −20 °C until use.

Microfluidic Analysis Platform. Biosensors were housed in a 3D printed chip, described in detail elsewhere.[10] Briefly, the 3D printed chip was fabricated in ABS White resist using an ULTRA 3SP printer. Biosensors were placed inside electrode holders,[9,10] which were printed using an Objet260 Connex printer that can print both hard and soft material in the same component. VeroWhitePlus (RGD835) and TangoBlack (FLX973) were used for the hard and soft materials, respectively. All parts were printed based on drawings generated in SolidWorks.

Wireless Recording Instrumentation. A wireless potentiostat and a data-recording mobile app were developed specifically for this application. The wireless potentiostat was implemented on a 2-layer printed circuit board (PCB) designed in-house using Eagle and manufactured by Newbury Electronics. The electronic components were purchased from Farnell and Mouser and were assembled onto the PCB in house, using the reflow soldering process. The PCB was powered by a small (50 × 37 × 10 mm^3) 3.7 V rechargeable lithium-ion battery (1.8 Ah, BAK). Data output by the

DOI: 10.1021/acs.analchem.9b03774
Anal. Chem. 2019, 91, 14631−14638

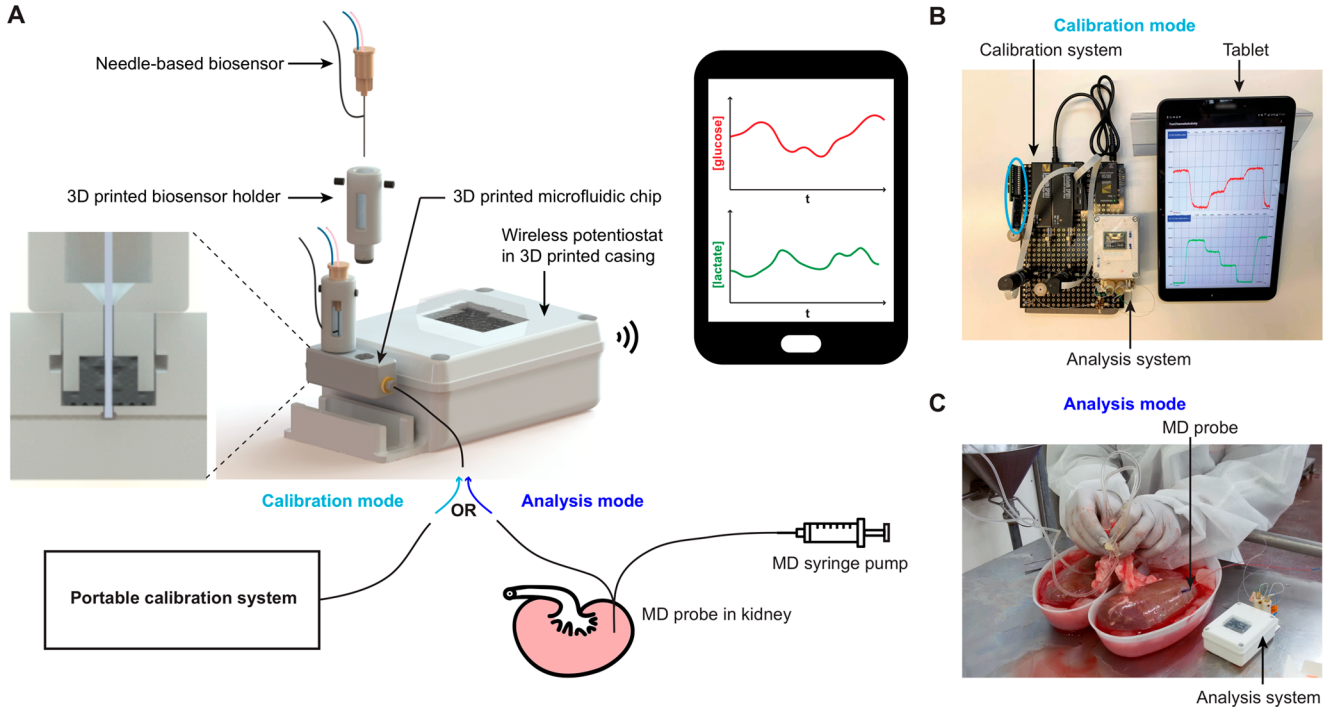

Figure 1. (A) Portable setup for monitoring transplant kidneys in transit. The analysis system consists of needle-based amperometric glucose and lactate biosensors controlled by a wireless two-channel potentiostat that transmits data to a tablet via Bluetooth. The signals recorded at the biosensors are transmitted and displayed on the tablet screen in real time using a custom-written Android app. The biosensors are inserted in the channel of a 3D printed microfluidic chip (see cross-section zoom-in) using 3D printed holders. The microfluidic chip is alternately connected to a portable calibration system (calibration mode) or to the outlet of a microdialysis probe that samples the kidney extracellular fluid (analysis mode). (B) Picture of the setup in calibration mode. The blue circle shows the wireless calibration controller PCB. (C) Picture of the setup in analysis mode while kidneys are undergoing cold flushing with preservation solution (photo used as an example in of in vivo clinical monitoring in ref 17. Published by the Royal Society of Chemistry).

potentiostat was digitized by the internal 10-bit analogue-to-digital converter of a microcontroller (ATmega328, Atmel) and sent using a Bluetooth module (Bluefruit EZ-Link, Adafruit) via serial communication. The schematics of the wireless potentiostat PCB is given in Figure S1. The recording mobile app was coded in Java using Android Studio and deployed on a SAMSUNG Galaxy Tab A 9.7" tablet.

Portable Calibration Platform. Biosensors were calibrated inside the microfluidic chip using the portable autocalibration board shown in Figure 1. This board was developed based on the microfluidic platform described elsewhere.[19] For this application, a wireless, battery-powered version of the system was developed. The autocalibration board consists of two 20 μL programmable syringe pumps (SPS01−020 LabSmith), one containing a glucose standard solution and the other a lactate standard solution. By mixing the two flows and varying the relative flow rates, a multipoint calibration can be carried out while keeping the overall flow rate constant at 2 μL/min. The pumps are each connected to a valve and a reservoir containing 1 mL of the solution. This allows the pumps to be continually refilled after each calibration cycle. To allow for wireless control of the autocalibration board, a wireless controller PCB was developed to plug into the board. The PCB was designed in-house using Altium and manufactured by Newbury Electronics. The complete board was assembled in-house. The wireless calibration controller PCB was mounted with a microcontroller (ATmega328, Atmel) and a Bluetooth module (Bluefruit EZ-Link, Adafruit) that received orders sent by a control mobile app developed specifically for this application. It was powered through the calibration board using a rechargeable 12 V lithium-polymer battery (20 Ah, Anker). The schematic of the wireless calibration controller PCB is given in Figure S2. The control mobile app was coded in Java using Android Studio and deployed on the same SAMSUNG Galaxy Tab A 9.7" tablet that runs the recording app. During sensor calibrations, both apps were run simultaneously. For ex vivo experiments, the sensors were continuously calibrated during the journey to the abattoir (typically 2 h). When the kidneys had been brought back to the laboratory, the sensors were calibrated again.

Kidney Protocol. The protocol for porcine kidney monitoring using microdialysis has been described in detail elsewhere.[27] A MAB 11.35.4 microdialysis probe (Microbiotech, 4 mm membrane, 6 kDa molecular weight cutoff) was used to monitor each kidney. In each case the probe was perfused prior to insertion and after removal at the end of each experiment to check for any blockages or leakages and to verify that the probe was functioning correctly during the whole monitoring period. The probes were perfused with T1 physiological solution (2.3 mM calcium chloride, 147 mM sodium chloride, 4 mM potassium chloride) at 2 μL/min using a portable syringe pump (CMA107 MDialysis). The outlet of the microdialysis probe was extended using a 50 cm length of fluorinated ethylene propylene (FEP) tubing (120 μm inner diameter) as this proved more practical for later packing of the organ in an ice box. Once the pig had been killed, the internal organs were removed and placed on a bench; a microdialysis probe was immediately inserted into the cortex of each kidney by a clinician and sutured in place (probes were in place

DOI: 10.1021/acs.analchem.9b03774
Anal. Chem. 2019, 91, 14631−14638

approximately 5 min after the pig was killed). The outlet of each microdialysis probe was connected to an analysis system to commence online monitoring. The kidneys were then dissected away from the other internal organs and left at room temperature for 40 min. This does not reflect a typical clinical scenario; however, it allowed for tissue levels to stabilize after probe insertion and for baseline measurements to be taken prior to cooling the kidney. Importantly, the longer warm ischemia time (WIT) used here also serves to more closely reflect more damaged kidneys such as those retrieved from ECD or uncontrolled DCD.

Following warm ischemia, the kidney was flushed with cold Soltran preservation solution (Baxter) for around 20 min to cool the kidney and to clear the vessels of blood to prevent clots from forming. After flushing, the kidneys were placed in a bag containing the preservation solution and in a box of ice to be transported back to the laboratory, which took ∼2 h on average. The kidneys were monitored in real time throughout the journey. Upon arrival in the lab, the kidneys were stored in the fridge overnight at 4 °C.

The following day the kidneys were preconditioned on a pulsatile preservation machine (Waters Medical) to investigate the effect of preservation treatments on tissue metabolite levels. The data from the preservation stage presented here is from a kidney that was treated with hypothermic machine perfusion (HMP) for 4 h with Belzer-MPS University of Wisconsin solution. Following the preservation stage, the kidneys were reperfused with oxygenated whole autologous blood at 37 °C for 2 h to mimic transplantation. Tissue glucose and lactate levels were monitored throughout preservation using our wireless analysis system. A total of six kidneys were monitored using this protocol.

Effect of Temperature on Microdialysis Sampling. For one kidney, an experiment was carried out to investigate the effect of temperature on microdialysis sampling. A second microdialysis probe was inserted in the cortex of the kidney as described above. In this case, the probe was perfused with an exogenous substance in order to look at the effects of temperature on the probe within the tissue, without introducing a substance that would interact with the tissue metabolism; the probe was perfused with 0.5 mM Fc solution at 2 μL/min. Monitoring the concentration of Fc in the dialysate at different temperatures gives a measure of the extraction fraction and hence the diffusion across the membrane.

The outlet of the probe was connected to a 3D printed microfluidic chip containing a needle electrode coated with a layer of hydrogel without enzyme (90 mg/mL BSA, 14.82 mg/mL PEG-DE, 1% glycerol in 10 mM PBS) to limit potential interferences, which was held at +0.5 V versus a Ag|AgCl reference electrode. The concentration of Fc in the dialysate outflow was measured in real time throughout the kidney preservation protocol on the second day, described above. The kidney temperature was measured throughout using a temperature probe (IT-14, Physitemp) connected to an in-house temperature sensor so that it could be correlated with the measured extraction fraction.

RESULTS AND DISCUSSION

Portable Analysis System. The portable analysis system was developed with the aim of monitoring tissue metabolite levels in nonlaboratory settings and in particular in transit. This required a robust miniaturized analysis system, securely incorporating glucose and lactate biosensors and a wireless calibration system to calibrate biosensors in transit. Figure 1A shows an overview of the components of the portable analysis system.

The analysis system consists of a 3D printed microfluidic chip housing glucose and lactate biosensors in 3D printed electrode holders. The holders are designed to secure the sensors in the chip, which is crucial for situations where the system moves around a lot, and to precisely position the sensor tips in the middle of the flow-stream.[10] Once the sensors have been fixed in holders, which can be done in advance, they can be easily and reliably replaced in the chip by a nonexpert, which is ideal for a clinical application.

A miniaturized two-channel wireless potentiostat was developed to control the amperometric biosensors (see Figure S1). The potentiostat was implemented on a PCB, small enough (3.5 × 5.1 cm^2) to travel with the kidney. A voltage difference of 0.7 V was applied between the working and reference electrodes using a voltage follower. Each channel was implemented with three different gain resistors (1, 5, and 10 GΩ) that could be selected using a manual switch, enabling the user to match the output current range to the biosensor response. This was particularly important as dialysate metabolite levels vary significantly between the different stages of the protocol. The potentiostat power was provided by a 3.7 V rechargeable battery. Data was sent in real time over Bluetooth to a custom-written Android app running on a tablet. The sampling rate was set to 10 samples/s but could be customized as required; the data was saved as soon as it was received by the tablet, and every second an average of the previous 10 samples was plotted on the app. This online filter could be customized by the user and meant that changes in metabolite levels could easily be seen as they occurred, even in high-noise environments.

As shown in Figure 1A the wireless potentiostat was encapsulated in a 3D printed casing to add protection. This was designed to secure both the potentiostat and the 3D printed chip and sensors in place; it consisted of a compact box (measuring 57 × 86 × 30 mm^3) to contain the potentiostat and a slot to hold the microfluidic chip. The lid incorporated a window above the gain switches to allow access once the lid was closed. This window was overlaid with a transparent waterproof cover to ensure that the system was splash-proof, which was a crucial requirement for use throughout surgery and in the abattoir. The microfluidic chip containing the biosensors was held securely in place in the custom-made slot providing a compact fully integrated system, ideal for monitoring transplant organs.

In order to be able to calibrate the analysis system away from the laboratory and in transit, a wireless autocalibration system was developed as shown in Figure 1B. The autocalibration system was made using LabSmith programmable microfluidic components and set up to carry out multipoint calibrations.[19] To implement a wireless version of this system, the calibration board was powered via a rechargeable battery, and a wireless calibration controller was developed to wirelessly control the components via Bluetooth. The wireless calibration controller interfaced with a custom-written Android app also running on the monitoring tablet, which allowed the user to send commands to the PCB controlling the autocalibration board by pressing buttons on the app graphical user interface. This wireless calibration system meant it was possible to calibrate the sensors on the way to the abattoir so that upon arrival the

DOI: 10.1021/acs.analchem.9b03774
Anal. Chem. 2019, 91, 14631−14638

analysis system was ready to use. Tubing was disconnected and reconnected to switch between calibration and analysis mode (Figure 1B,C, respectively).

The whole system was validated in transit while traveling to the abattoir to collect kidneys. It was packed in a bag and taken in a taxi, on the train, and on the underground while automatically carrying out repeated calibrations. An excerpt of data from this journey is shown in Figure 2A (for data from a 3 h long journey, see Figure S3); glucose and lactate biosensors were repeatedly calibrated from 0 to 2 mM in four steps. No drop-out in the signal was seen, and the system demonstrated high signal fidelity even in high-noise environments, proving its suitability for clinical monitoring. The corresponding calibration curves are shown in Figure 2B demonstrating the robustness and reproducibility of the system in its true conditions of use. For calibration curves of multiple biosensors, see Figure S4.

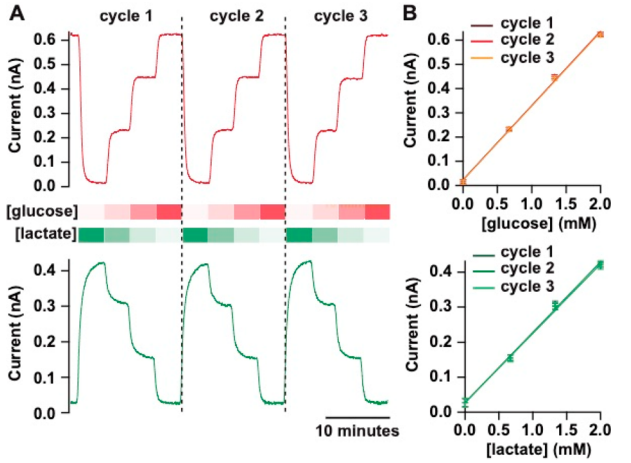

Figure 2. Typical glucose (red) and lactate (green) biosensor calibration traces recorded in transit. The four following concentration steps were generated repeatedly at 2 μL/min using the portable calibration system: 0, 0.66, 1.34, and 2 mM for glucose and 2, 1.34, 0.66, and 0 mM for lactate. Data are shown for three consecutive calibration cycles. (A) Online-recorded currents sampled at 10 Hz and smoothed with a Savitzky−Golay 101-point filter. (B) Corresponding calibration curves for each repeat, fitted with a straight line. Markers and error bars represent mean and sd of 1 min measurements.

Continuous Kidney Monitoring in Transit. In a proof-of-concept study to demonstrate the potential of this system for clinical monitoring in transit, the portable analysis system was used to monitor tissue glucose and lactate levels in porcine kidneys ex vivo in real time during organ retrieval and in transit back to the laboratory. For each pig, both kidneys were monitored using two portable systems (one for each kidney).

A microdialysis probe was inserted into the cortex of each kidney immediately after the internal organs had been removed from the pig, as shown in Figure 3C(i). The cortex was chosen as we have previously shown that it is the most metabolically active region.[17] At this point, each analysis system was disconnected from its calibration board and connected to the outlet of one of the two microdialysis probes to commence online monitoring. The kidneys were subjected to 40 min of warm ischemia at room temperature during which time they were dissected away from the other internal organs. After this time, they were flushed with a cold Soltran preservation solution as shown in Figure 3C(ii). Finally, each kidney was placed in an ice box for transport back to the laboratory. As the biosensors are functionalized with enzymes, which have optimal working temperatures, and rely on diffusion and chemical reactions to give a signal, their sensitivity is likely to decrease if the temperature is lowered. To determine whether the analysis system could be placed inside the ice box, experiments were carried out to investigate whether this reduction in sensor sensitivity caused by lowering the temperature was predictable; however, the effect was found to be variable, and therefore, it would not be possible to reliably account for this (see Figure S5). The low temperature was not found to have an effect on the analysis system when it was placed outside the ice box as shown in Figure S6. Therefore, as shown in Figure 3C(iii), the analysis system was instead placed outside of the ice box to avoid the cold temperatures affecting the biosensor response.

Figure 3A shows an example of continuous glucose and lactate dialysate levels measured in a kidney from organ retrieval to transport back to the laboratory. The microdialysis data has been time-aligned with clinical events. A rise in levels of both glucose and lactate can be seen clearly upon insertion of the microdialysis probe. The levels are initially changeable, as the organs were being dissected, resulting in movement of the probe in the tissue. During this time dialysate glucose levels were between 0.1 and 0.3 mM and lactate levels were between 0.8 and 1.9 mM. After surgery on the organs was completed, the signals stabilized and gradually decreased down to 50 μM for glucose and 500 μM for lactate. A large transient increase in lactate and a small transient decrease in glucose is seen when cold flushing of the organ begins. As the changes are in opposite directions, this cannot be an artifact of probe recovery.[28] These changes are attributed to the flushing of the organ causing redistribution of local lactate to the probe from nearby tissue and glucose being flushed out. As a result of cold flushing, levels of both metabolites decrease steeply until they stabilize at 20 μM for glucose and 200 μM for lactate. Upon placing the kidney in the ice box the levels continue to gradually decrease, indicating that tissue metabolism is shutting down due to the cold temperatures; after 30 min in the ice box, glucose levels are below 12.2 μM (three times the standard deviation (sd) of the signal). Despite the challenging environment of the abattoir, using this robust analysis system we were able to measure metabolite tissue levels during these crucial first stages of organ procurement for the first time.

Six kidneys were monitored from retrieval and in transit back to the laboratory using our portable analysis system. Figure 3B shows a box plot summarizing the dialysate glucose and lactate levels in these six kidneys at key time-points during the monitoring period. The glucose signal for one kidney was rejected as the glucose biosensor output was very noisy, and the levels were indistinguishable from noise. The lactate levels started high in all cases and decreased over the monitoring period. Paired statistical analysis using a Wilcoxon signed-rank test shows a significant decrease in the dialysate lactate concentration during warm ischemia as well as when the kidneys were flushed with cold preservation solution. Dialysate glucose levels also appear to decrease during warm ischemia, although this change was not significant. During cold storage, glucose levels were not distinguishable from zero, suggesting a low energy supply to the tissue, or potentially high glucose use. The low and stable lactate levels at the same time indicate that

DOI: 10.1021/acs.analchem.9b03774
Anal. Chem. 2019, 91, 14631−14638

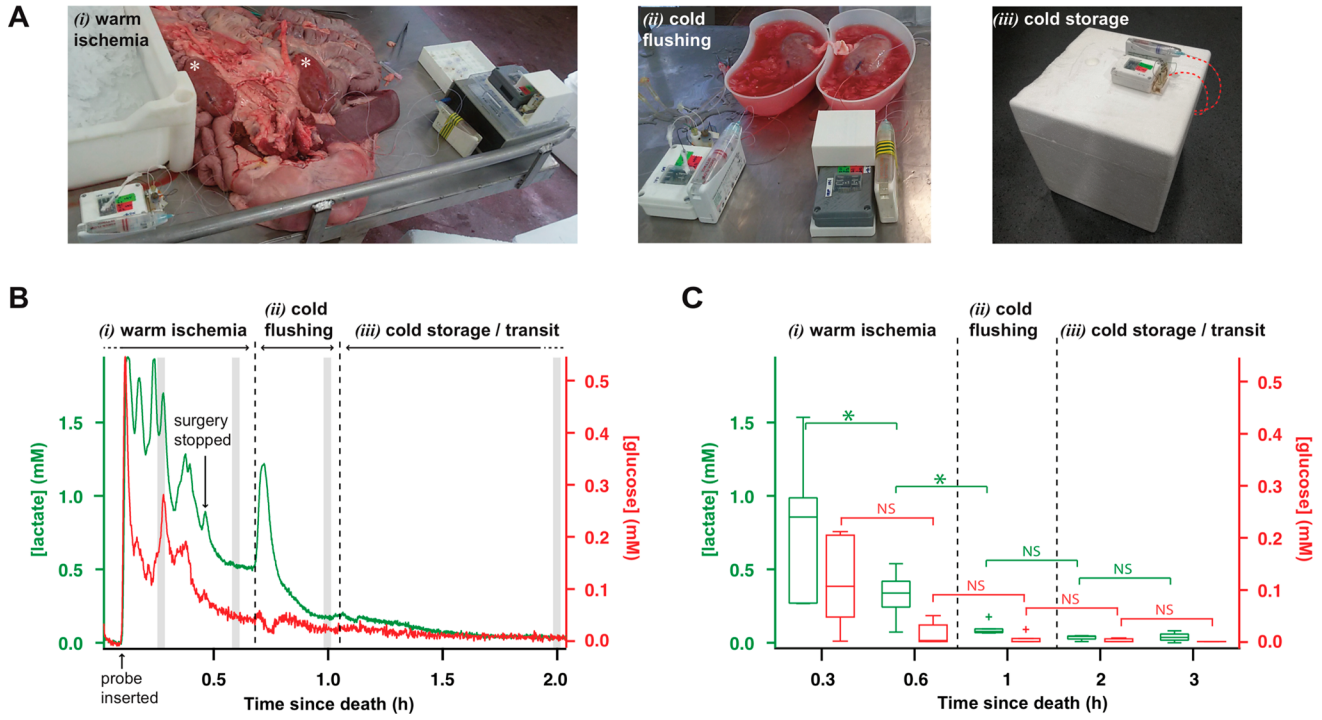

Figure 3. (A) Pictures of the kidney monitoring setup (i) during passive warm ischemia immediately following organ retrieval before dissection away from the other internal organs (kidneys indicated by white asterisks), (ii) during cold flushing, and (iii) during cold storage for one kidney during transit. (B) Dialysate glucose (red) and lactate (green) levels of a porcine kidney recorded online immediately after retrieval and during transit for a kidney subjected to passive warm ischemia, cold flushing, and cold storage. Online data was sampled at 10 Hz and smoothed with a Savitzky-Golay 201-point filter. Gray strips indicate the 2 min intervals at which the data was averaged to give the box plot shown in (C). (C) Dialysate glucose (red) and lactate (green) levels for six kidneys at five time-points over the 3 h following pig death. Box plots show median levels and interquartile range. Whiskers indicate 10th and 90th percentiles. Wilcoxon signed-rank test (lactate $n = 6$, glucose $n = 5$, as for one kidney the glucose levels were so low they were indistinguishable from noise), significance: $^*p < 0.05$, NS = not significant.

glucose use is low, and the tissue was in a slow and well-regulated metabolic state.

Monitoring Longer Clinical Interventions. Once the kidneys had been brought back to the laboratory, they were stored in the fridge overnight before preservation interventions were investigated the following day. In some cases online kidney monitoring continued over this period of cold storage, for a duration of 12 h. During this time, dialysate glucose levels were below the detection limit of our monitoring system. Dialysate lactate levels were also low and stable at 63 ± 9 μM (mean ± sd) over the 12 h time period. This further indicates that at these temperatures tissue metabolism is slow and well regulated.

The following day the kidneys were preconditioned for 4 h on a perfusion machine. Following this preconditioning phase, the kidneys were warm perfused with autologous whole blood to mimic transplantation. Figure 4A shows an example of dialysate glucose and lactate levels during the end of the preconditioning phase and during reperfusion for a kidney that was preconditioned with HMP. There is a clear increase in dialysate levels of both glucose and lactate when the kidney goes from the cold preservation phase to reperfusion (from 0.12 ± 0.03 mM to 3.70 ± 0.46 mM for glucose and from 0.21 ± 0.03 mM to 2.41 ± 0.12 mM for lactate, mean ± sd on a 10 min interval immediately before and after the start of reperfusion, corresponding to a 30-fold and 11-fold increase, respectively). Whereas during HMP, levels of glucose and lactate remained fairly constant, during reperfusion, glucose levels slowly decrease while lactate levels slowly increase; this

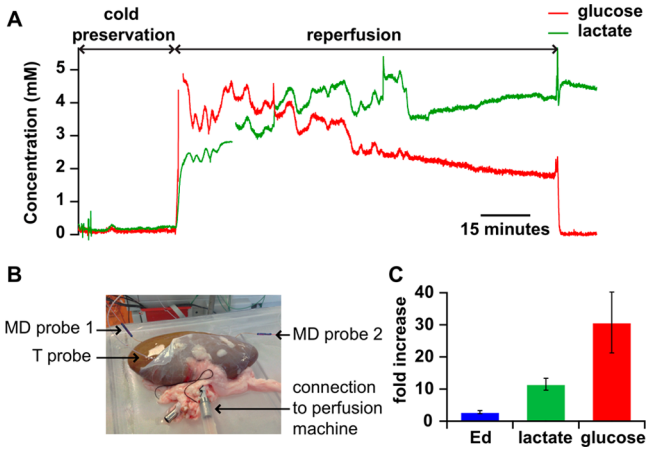

Figure 4. (A) Dialysate glucose (red) and lactate (green) levels recorded from a kidney subjected to cold preservation and reperfusion with autologous blood. Online data sampled at 10 Hz and smoothed with a Savitzky-Golay 201-point filter. (B) Picture of a kidney with two microdialysis (MD) probes inserted (one for metabolite sampling and one for extraction fraction measurements) and a temperature probe during HMP. (C) Fold increase in the microdialysis probe ex vivo Fc extraction fraction (E_d) and in the lactate and glucose dialysate concentrations due to the transition from cold preservation to reperfusion. For glucose and lactate, mean values and sd (error bars) are calculated over a 10 min interval (over 6000 data points) immediately before and after the start of reperfusion and for E_d mean and sd are calculated over a 10 min interval for HMP and reperfusion (over 6000 data points).

DOI: 10.1021/acs.analchem.9b03774
Anal. Chem. 2019, 91, 14631−14638

indicates that tissue metabolism has resumed and the kidney is respiring anaerobically in order to meet the increased energy demands of the tissue. This demonstrates the potential of the analysis system not just for monitoring situations that require portability but also for monitoring clinical interventions taking place over multiple days.

An increase in dialysate levels between the phases of HMP and reperfusion is to be expected as the kidney is warmed, increasing recovery across the membrane. An experiment was therefore carried out to investigate whether this could explain the increased levels of glucose and lactate seen in Figure 4A. This was done using an exogenous compound, Fc, to make it possible to distinguish the effect of temperature on diffusion within the tissue and across the membrane from the effect on tissue metabolism and cellular exchanges. In this experiment, Fc was perfused through a second microdialysis probe positioned in the kidney as shown in Figure 4B. The concentration of Fc in the dialysate was measured to calculate how much Fc had diffused out of the probe, i.e., the extraction fraction. The rate of diffusion of Fc across the membrane into the tissue can provide a first approximation of the probe recovery from the tissue, although these parameters have been shown not to be exactly equivalent.[29−31] Figure 4C shows the extraction fraction during HMP and reperfusion. This data shows that the extraction fraction increased from 6% during cold perfusion at 8 °C to 17% during warm perfusion at 33 °C, corresponding to a 2.8-fold increase. This is considerably less than the increase in metabolite levels seen in Figure 4A, indicating that although some of this increase will be due to an increase in probe recovery, a large proportion of it is caused by physiological changes in the tissue itself caused by the change in treatment.

CONCLUSION

We have demonstrated the first example of using a portable analysis system to monitor physiological levels of tissue metabolites in real time from organ retrieval right through to preservation and during transportation. We have demonstrated the capabilities of the analysis system for measuring changes in the levels of glucose and lactate in a kidney during each stage of organ procurement, from warm to cold ischemia, and during preservation, indicating the huge potential of this device for real-time monitoring and evaluation of transplant organs as they are transported from donor to recipient hospitals. Tissue concentrations of glucose represent a balance between supply from the blood (or other perfusing media) and local tissue utilization by metabolism. Tissue lactate concentration increases reflect lack of oxygen, though ultimately they can become limited by glucose supply, hence the need to measure both. These measurements in challenging environments and in transit were made possible due to the portability and robustness of the analysis system and due to the inclusion of a portable calibration system. This miniaturized analysis system has vast potential for use in other clinical microdialysis applications where size, portability, and robustness are important considerations. For instance, this analysis system would be ideal in a crowded theater environment where the monitoring device must be compact and robust; this system would remove the need for the long connection tubing that is often required, which usually leads to long delays and loss of temporal resolution.[10,11] We have also demonstrated the durability and reliability of the system in monitoring over multiple days. Future work will focus on correlating these results with clinical measurements of kidney function in order to establish markers of tissue health and potential predictors of kidney viability. We are also investigating surface probes with greater tissue coverage.

ASSOCIATED CONTENT

Supporting Information

The Supporting Information is available free of charge on the ACS Publications website at DOI: 10.1021/acs.analchem.9b03774.

Wireless potentiostat schematic (S1), wireless calibration controller PCB schematic (S2), stability of biosensor response in transit (S3), variability across multiple biosensor responses (S4), effect of temperature on biosensor sensitivity (S5), and effect of temperature at the microdialysis probe on temperature at the biosensors (S6) (PDF)

AUTHOR INFORMATION

Corresponding Author

*E-mail: m.boutelle@imperial.ac.uk.

ORCID

Sally A. N. Gowers: 0000-0002-2407-2266

Martyn G. Boutelle: 0000-0003-1332-3442

Author Contributions

‖I.S. and S.G. contributed equally to this work.

Notes

The authors declare no competing financial interest.

ACKNOWLEDGMENTS

We would like to thank EPSRC (I.S. PhD studentship, S.G.) and Wellcome Trust DOH (HICF-0510-080) for funding. We would also like to thank the Freemasons Foundation of New Zealand through the Royal Society of New Zealand-Rutherford Foundation (MB).

REFERENCES

(1) U. S. Department of Health & Human Services. *Organ Procurement & Transplantation Network*, 2019.

(2) Hoogland, E. R. P.; Snoeijs, M. G. J.; Winkens, B.; Christaans, M. H. L.; Van Heurn, L. W. E. *Am. J. Transplant.* **2011**, *11* (7), 1427−1434.

(3) Mallon, D. H.; Summers, D. M.; Bradley, J. A.; Pettigrew, G. J. *Transplantation* **2013**, *96* (10), 885−889.

(4) Locke, J. E.; Segev, D. L.; Warren, D. S.; Dominici, F.; Simpkins, C. E.; Montgomery, R. A. *Am. J. Transplant.* **2007**, *7* (7), 1797−1807.

(5) Port, F. K.; Bragg-Gresham, J. L.; Metzger, R. A.; Dykstra, D. M.; Gillespie, B. W.; Young, E. W.; Delmonico, F. L.; Wynn, J. J.; Merion, R. M.; Wolfe, R. A.; Held, P. J.; et al. *Transplantation* **2002**, *74* (9), 1281−1286.

(6) Ojo, A. O.; Hanson, J. A.; Okechukwu, C. N.; Wolfe, R. A.; Leichtman, A. B.; Agodoa, L. Y.; Kaplan, B.; Port, F. K. *J. Am. Chem. Soc. Nephrol.* **2001**, *12*, 589−597.

(7) Summers, D. M.; Watson, C. J. E.; Pettigrew, G. J.; Johnson, R. J.; Collett, D.; Neuberger, J. M.; Bradley, J. A. *Kidney Int.* **2015**, *88* (2), 241−249.

(8) Booth, M. A.; Gowers, S. A. N.; Leong, C. L.; Rogers, M. L.; Samper, I. C.; Wickham, A. P.; Boutelle, M. G. *Anal. Chem.* **2018**, *90* (1), 2−18.

(9) Gowers, S. A. N.; Curto, V. F.; Seneci, C. A.; Wang, C.; Anastasova, S.; Vadgama, P.; Yang, G. Z.; Boutelle, M. G. *Anal. Chem.* **2015**, *87* (15), 7763−7770.

DOI: 10.1021/acs.analchem.9b03774
Anal. Chem. 2019, 91, 14631−14638

(10) Viggiano, A.; Marinesco, S.; Pain, F.; Meiller, A.; Gurden, H. *J. Neurosci. Methods* **2012**, *206* (1), 1−6.
(11) Rogers, M. L.; Leong, C. L.; Gowers, S. A.; Samper, I. C.; Jewell, S. L.; Khan, A.; McCarthy, L.; Pahl, C.; Tolias, C. M.; Walsh, D. C. *J. Cereb. Blood Flow Metab.* **2017**, *37* (5), 1883.
(12) Wang, M.; Roman, G. T.; Schultz, K.; Jennings, C.; Kennedy, R. T. *Anal. Chem.* **2008**, *80* (14), 5607−5615.
(13) Wang, D.; Li, X.; Jiang, Y.; Jiang, Y.; Ma, W.; Yu, P.; Mao, L. *ACS Chem. Neurosci.* **2019**, *10* (5), 2576−2583.
(14) Varner, E. L.; Leong, C. L.; Jaquins-Gerstl, A.; Nesbitt, K. M.; Boutelle, M. G.; Michael, A. C. *ACS Chem. Neurosci.* **2017**, *8* (8), 1779−1788.
(15) Scott, D. E.; Willis, S. D.; Gabbert, S.; Johnson, D.; Naylor, E.; Janle, E. M.; Krichevsky, J. E.; Lunte, C. E.; Lunte, S. M. *Analyst* **2015**, *140* (11), 3820−3829.
(16) Nandi, P.; Lunte, S. M. *Anal. Chim. Acta* **2009**, *651*, 1−14.
(17) Hamaoui, K.; Gowers, S.; Damji, S.; Rogers, M.; Leong, C. L.; Hanna, G.; Darzi, A.; Boutelle, M.; Papalois, V. *J. Surg. Res.* **2016**, *200* (1), 332−345.
(18) Gowers, S. A. N.; Hamaoui, K.; Cunnea, P.; Anastasova, S.; Curto, V. F.; Vadgama, P.; Yang, G.-Z.; Papalois, V.; Drakakis, E. M.; Fotopoulou, C.; et al. *Analyst* **2018**, *143* (3), 715−724.
(19) Gowers, S. A. N.; Rogers, M. L.; Booth, M. A.; Leong, C. L.; Samper, I. C.; Phairatana, T.; Jewell, S. L.; Pahl, C.; Strong, A. J.; Boutelle, M. G. *Lab Chip* **2019**, *19*, 2537.
(20) Schultz, K. N.; Kennedy, R. T. *Annu. Rev. Anal. Chem.* **2008**, *1*, 627−661.
(21) Watson, C. J.; Venton, B. J.; Kennedy, R. T. *Anal. Chem.* **2006**, *78* (5), 1391−1399.
(22) Wang, M.; Roman, G. T.; Perry, M. L.; Kennedy, R. T. *Anal. Chem.* **2009**, *81* (21), 9072−9078.
(23) Nandi, P.; Scott, D. E.; Desai, D.; Lunte, S. M. *Electrophoresis* **2013**, *34* (6), 895−902.
(24) Rogers, M. L.; Feuerstein, D.; Leong, C. L.; Takagaki, M.; Niu, X.; Graf, R.; Boutelle, M. G. *ACS Chem. Neurosci.* **2013**, *4*, 799−807.
(25) Patel, B. A.; Rogers, M.; Wieder, T.; O'Hare, D.; Boutelle, M. G. *Biosens. Bioelectron.* **2011**, *26* (6), 2890−2896.
(26) Vasylieva, N.; Barnych, B.; Meiller, A.; Maucler, C.; Pollegioni, L.; Lin, J.; Barbier, D.; Marinesco, S. *Biosens. Bioelectron.* **2011**, *26*, 3993−4000.
(27) Gowers, S. A. N.; Hamaoui, K.; Vallant, N.; Hanna, G. B.; Darzi, A.; Casanova, D.; Papalois, V.; Boutelle, M. G. *Anal. Methods* **2018**, *10* (44), 5273−5281.
(28) Parkin, M. C.; Hopwood, S. E.; Boutelle, M. G.; Strong, A. J. *TrAC, Trends Anal. Chem.* **2003**, *22* (8), 487−497.
(29) Peters, J. L.; Michael, A. C. *J. Neurochem.* **1998**, *70* (2), 594−603.
(30) Yang, H.; Peters, J. L.; Michael, A. C. *J. Neurochem.* **1998**, *71* (2), 684−692.
(31) Lu, Y.; Peters, J. L.; Michael, A. C. *J. Neurochem.* **1998**, *70* (2), 584−593.

DOI: 10.1021/acs.analchem.9b03774
Anal. Chem. 2019, 91, 14631−14638